

# Bubbling laws in a glass furnace

X. Chavanne, J.-M. Flesselles, F. Pigeonneau

*Saint-Gobain Recherche, 39 quai Lucien Lefranc, 93303 Aubervilliers cedex France*

Bubblers are commonly used in glass furnaces in order to enhance convective motions. Despite extensive studies, bubble formation from an orifice has not been described by a single law. Usually the formed bubble volume depends at least on two parameters: the viscosity and the gas flow rate in dimensionless form. By reconsidering available models, we have derived a single parameter law to describe bubble formation for different gas flow rates and fluids. Two regimes appear, namely the viscous and inertial regimes, depending on the value of this parameter.

## Introduction

Bubbling from an orifice at the bottom play an important role to improve the mass, heat and momentum transfers in different applications (cell oxygenation, water cleansing, gas phased polymerization, in molten steel bath, ...). In glass furnaces rows of bubblers blow up nitrogen gas or air in molten silicate through an orifice of diameter  $d_{or}$ , in order to improve the glass quality at the output. Bubbling conditions often correspond to a constant volume flow rate  $Q$ .

It is important to know the bubble volume  $V$  at the end of the formation process, as  $V$  drives the bubble velocity and the flow in surrounding liquid. Bubble formation has received much theoretical as well as experimental and numerical attention. In the next section we summarize the work done on this topic and present the resulting equation that controls the volume of the bubble  $V$  just before the detachment. In the following section, from physical considerations, we deduce a simpler form, that may be useful for many applications and glass making in particular.

## The existing law of bubbling

Different theoretical works <sup>1 2 3 4</sup> have established an equation governing the bubble volume inside a fluid of dynamical viscosity  $\eta$ , of density  $\rho$  and of surface tension  $\sigma$ . The equation derives from a momentum balance applied to the bubble and from a detachment criterion based on experimental observations. The forces in play on the bubbles are the following:

- Buoyancy force. The main upward force is  $\rho g V$ . Gas density is neglected.
- Gas momentum force. This upward force is negligible in most cases.
- Tension surface force. This force maintains the bubble down along the surface contact line on the orifice nozzle. Its expression is  $\pi d_{or} \sigma$ .
- The drag force exerted by the liquid on the bubble during its expansion. Its general form is  $\frac{1}{2} \rho W^2 \pi D^2 / 4 C_d$  where  $W$  is the bubble velocity,  $D$  its diameter and  $C_d$  the drag coefficient. At the detachment  $W$  is approximated<sup>5</sup> by  $(3D/4)(Q/V)$  while  $C_d$  expression is  $24/Re + 1$  from experimental considerations.  $Re$  is the bubble based

Reynolds number,  $\rho W D / \eta$ . The first term of Cd corresponds to the viscous part of the drag while the second term is related to the turbulent drag.

- The inertia force or added mass contribution. It is the force resulting from accelerating an inviscid liquid. Its expression is  $\alpha \rho \gamma$  where  $\alpha$  is a dimensionless parameter and  $\gamma$  is the bubble acceleration. For a sphere moving close to a wall  $\alpha$  is approximately 11/16 while  $\gamma$  is approximated<sup>5</sup> by  $W Q / V$ .

By sorting out the different terms, the equation results in:

$$\rho g V \approx \pi d_{or} \sigma + \frac{45}{8\pi} \left( \frac{\pi^2}{36} \right)^{1/3} \frac{\rho Q^2}{V^{2/3}} + \frac{81}{\pi} \left( \frac{\pi^2}{36} \right)^{2/3} \frac{\eta Q}{\rho V^{1/3}} \quad (1)$$

This equation gives an implicit form to determine V. V is a function of Q but also g,  $\rho$ ,  $\eta$ ,  $d_{or}$  and  $\sigma$ .  $d_{or}$  and  $\sigma$  appear only by their product in the equation; hence only  $d_{or} \sigma$  is considered instead of the two parameters. To reduce further the number of parameters one can use a dimensional analysis as done by Clift et al.<sup>6</sup>. They have chosen g,  $\rho$  and  $d_{or} \sigma$  to put V, Q and  $\eta$  in dimensionless form:

$$V' = V g \frac{\rho}{d_{or} \sigma} \quad Q' = Q g^{1/3} \left( \frac{\rho}{d_{or} \sigma} \right)^{5/6} \quad Oh = \frac{\eta}{(\rho d_{or} \sigma)^{1/2}} \quad \text{the Ohnesorge number.}$$

Equation (1) becomes:

$$V' \approx \pi + \frac{45}{8\pi} \left( \frac{\pi^2}{36} \right)^{1/3} \frac{Q'^2}{V'^{2/3}} + \frac{81}{\pi} \left( \frac{\pi^2}{36} \right)^{2/3} \frac{Oh Q'}{V'^{1/3}} \quad (2)$$

In the  $V'$   $Q'$  diagram of fig. 1 are plotted curves for different Oh, deduced from (2) by numerical resolution.

From equation (2) one can derive the different asymptotic regimes<sup>5</sup>. Each regime corresponds to the balance of the left-hand side of (2) by one of the right-hand side terms:

- capillary regime:  $V'_c = \pi$  observed at low  $Q'$  and low Oh
- viscous regime:  $V'_v = 6.0 (Oh Q')^{3/4}$  observed at intermediate  $Q'$  and large Oh
- inertial regime:  $V'_i = 1.1 Q'^{6/5}$  observed at large  $Q'$  and low and moderate Oh

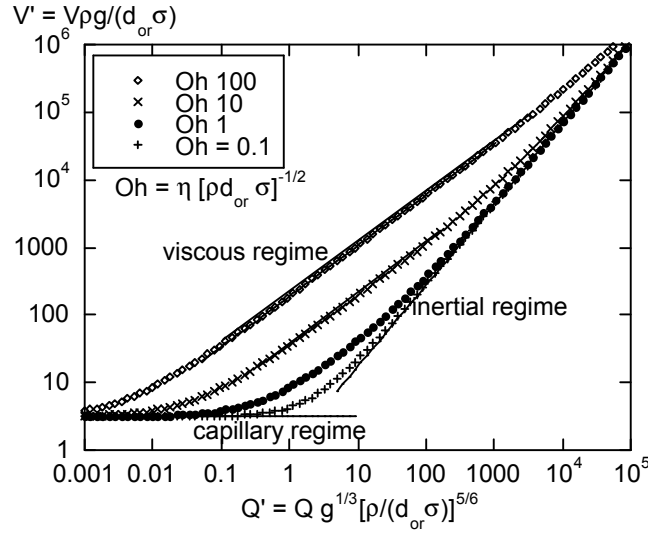


Fig 1. Points (V',Q') for different Oh deduced from the bubble volume V governing equation in dimensionless form (2). Different regimes of bubbling are highlighted.

Although in a more convenient form than equation (1) there are still too many parameters to determine at quick glance in which regime a bubbler falls. At the next paragraph parameter numbers are reduced by a further twist in the dimensional analysis.

#### A new dimensionless parametrization

The same procedure, which allows passing from (1) to (2), is again applied here but with a different set of parameters to make (1) dimensionless. The change arises from the fact that, in the bubbler case, the tension surface term is negligible. Typically for bubblers the normal gas flow rate is about 100 N l/h (normal condition is 0°C and 1 atm), the orifice diameter  $d_{or}$  is about 1 mm. Bubble emission rate is around 30 per min. For flat glass the viscosity  $\eta$  at 1525 K is about 50 Pas,  $\rho$  is 2500 kg.m<sup>-3</sup>. Hence V' value for the different regimes is about:

$$V'_c = \pi \quad V'_i \approx 460 \quad V'_v \approx 4900$$

One can see that the capillary term is negligible with respect to the others.  $d_{or}\sigma$  does not play a role in the physical mechanism of the phenomena. A better set of parameters is then g,  $\rho$ ,  $\eta$ . For simplification purpose the cinematic viscosity ( $\nu = \eta\rho^{-1}$ ) is also introduced. This yields the following dimensionless numbers:

$$V^* = V \frac{g}{\nu^2} \quad Q^* = Q \frac{g^{1/3}}{\nu^{5/3}}$$

Equation (1) rewrites:

$$V^* \approx \frac{\pi}{Oh^2} + \frac{45}{8\pi} \left( \frac{\pi^2}{36} \right)^{1/3} \frac{Q^{*2}}{V^{*2/3}} + \frac{81}{\pi} \left( \frac{\pi^2}{36} \right)^{2/3} \frac{Q^*}{V^{*1/3}} \quad (3)$$

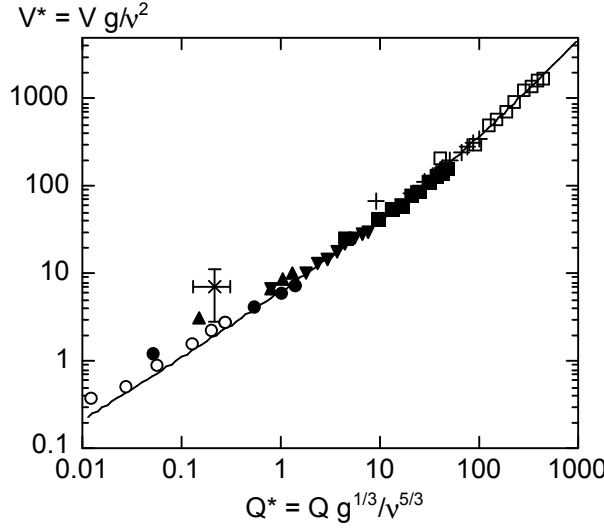


Fig. 2: Points  $(V^*, Q^*)$  from equation (3) for large Oh ( $Oh=10$ ) along with experimental data; ( $\square$ ) glycerol water mixture 43 mPas (+) glycerol water mixture 105 mPas ( $\blacksquare$ ) glycerol water mixture 165 mPas ( $\blacktriangledown$ ) glycerol water mixture 475 mPas ( $\blacktriangle$ ) glycerol water mixture 800 mPas (x) bubbler ( $\bullet$ ) bubbler model 7.4 Pas ( $\circ$ ) bubbler model 19 Pas.

In a similar way as the previous section, points from (3) are plotted in the  $V^* Q^*$  diagram of fig. 2. from physical considerations. Various experimental data are also reported. The first series was obtained by air injection within different glycerol water mixtures<sup>5</sup>. The second series concerns bubbler models working nearly at room temperature. In the previous framework  $(Q', Oh)$  points were scattered among different curves depending on the fluid viscosity. In the new framework  $(Q^*)$  points line up along the same curve well fitted by equation (3). A bubbler working point is also reported with its large error bars. The vicinity of other bubblers may modify the volume  $V$  of bubbles, and induce a shift from equation (3).

The different asymptotic regimes rewrite:

- capillary regime:  $V_c^* = \pi Oh^{-2}$  observed at low  $Q^*$  and low Oh
- viscous regime:  $V_v^* = 6.0 Q^{*3/4}$  observed at low  $Q^*$
- inertial regime:  $V_i^* = 1.1 Q^{*6/5}$  observed at large  $Q^*$

It is interesting to draw the boundary between the different regimes in the  $Q^* Oh$  diagram (fig.3):

- A limit between the two last regimes deduced from  $V_v^* = V_i^*$  is  $Q_{vi}^* = 44$
- A limit between the first and last regimes deduced from  $V_c^* = V_i^*$  is  $Q_{ci}^* = 2.4 Oh^{-5/3}$
- A limit between the two first regimes deduced from  $V_c^* = V_v^*$  is  $Q_{cv}^* = 0.42 Oh^{-8/3}$

The triple point where all the boundary lines met is  $Q^*_t = 44$  and  $Oh_t = 0.175$

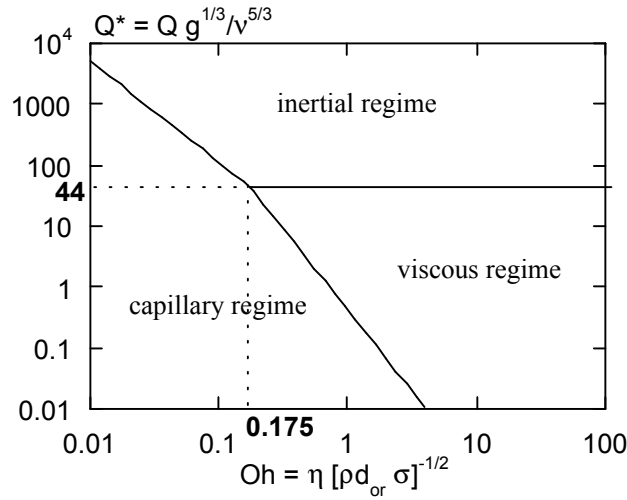


Fig. 3: Different bubbling regimes in the  $Q^*$   $Oh$  diagram

### Conclusion

In this article we suggest a new form of the equation governing the bubble volume  $V$  at its detachment. This form is convenient for bubbling applications where surface tension is negligible. This is the case of bubblers in a glass furnace. The volume in dimensionless form,  $V^* = Vg\nu^{-2}$  depends only on  $Q^* = Qg^{1/3}\nu^{-5/3}$ . Available experimental data support this new form.

We thank Y. Sion (SGCV, Chalon/Saône), R. Jacques, B. Palmieri and M. Rattier (SGR) for providing us with experimental data.

<sup>1</sup> J. F. Davidson and B. O. Schüller, Trans. Instn. Chem. Engrs **38**, p. 144-154 (1960).

<sup>2</sup> R. Kumar and N. R. Kuloor, Advances in Chemical Engineering **8**, p. 256-368 (1970).

<sup>3</sup> K. Ruff, Chemie Ing. Techn. **44**, p. 1360-1366 (1972).

<sup>4</sup> E. S. Gaddis and A. Vogelpohl, Chemical Engineering Science **41**, p. 97-105 (1986).

<sup>5</sup> P. Snabre and F. Magnifotcham, Euro. Phys. J. B **4**, p. 369-377 (1998).

<sup>6</sup> R. Clift, J. R. Grace and M. E. Weber, in *Bubbles, Drops and Particles* (Academic Press, New York, 1978).